We are IntechOpen, the world's leading publisher of Open Access books Built by scientists, for scientists

6,900
Open access books available

185,000
International authors and editors

200M
Downloads

Our authors are among the

154
Countries delivered to

TOP 1%
most cited scientists

12.2%
Contributors from top 500 universities



WEB OF SCIENCE™

Selection of our books indexed in the Book Citation Index in Web of Science™ Core Collection (BKCI)

Interested in publishing with us?
Contact book.department@intechopen.com

Numbers displayed above are based on latest data collected.
For more information visit www.intechopen.com



12

Reduced-Complexity PAPR Minimization Schemes for MC-CDMA Systems

Mariano García Otero and Luis A. Paredes Hernández
Universidad Politécnica de Madrid
Spain

1. Introduction

Multicarrier Code-Division Multiple Access (MC-CDMA) (Hara & Prasad, 1997), which is based on a combination of an CDMA scheme and Orthogonal Frequency Division Multiplexing (OFDM) signaling (Fazel & Kaiser, 2008), has attracted much attention in forthcoming mobile communication systems, because of its intrinsic spectrum efficiency and interference suppression capabilities. In MC-CDMA, information symbols of many users are spread using orthogonal codes and combined in the frequency domain; this results in a relatively low symbol rate and thus non-selective fading in each subcarrier.

However, one main drawback of any kind of multicarrier modulation is the inherent high value of the Peak-to-Average Power Ratio (PAPR) of the transmitted signals, because they are generated as an addition of a large number of independent signals. If low power consumption at the transmitter is a strict requirement, one would like the RF High Power Amplifier (HPA) to operate with a low back-off level (i.e. with operation point near saturation state); as a consequence of this, signal peaks will frequently enter the nonlinear part of the input-output characteristic of the HPA, thus causing severe nonlinear artifacts on the transmitted signals such as intermodulation distortion and out-of-band radiation. Therefore, reducing the PAPR is crucial in multicarrier systems, especially when transceivers are fed by batteries (such as in mobile devices), because of the intrinsic limitations in power consumption.

There has been a lot of research work about PAPR reduction techniques in multicarrier systems. Among these, we have clipping and filtering schemes (Li & Cimini, 1997), block coding algorithms (Jones et al., 1994), the Partial Transmit Sequences (PTS) (Cimini & Sollenberger, 2000; Jayalath & Tellambura, 2000), and Selected Mapping (SLM) approaches (Bäuml et al., 1996; Breiling et al., 2001), and the Tone Reservation (TR) (Tellado & Cioffi, 1998), and the Tone Injection (TI) techniques (Han et al., 2006). In general, reducing the PAPR is always done either at the expense of distorting the transmitted signals, thus increasing the BER at the receiver, or by reducing the information data rate, usually because high PAPR signals are somehow discarded and replace by others with lower PAPR before been transmitted.

All the previously mentioned methods have been originally proposed for single-user multicarrier schemes such as OFDM. Although most of them are also applicable with minor modifications to MC-CDMA systems (Ruangsurat & Rajatheva, 2001; Ohkubo & Ohtsuki, 2002), other families of algorithms can be developed after carefully considering the different

structure of the generated MC-CDMA signals. Between these, probably the most popular are those based on dynamically selecting an "optimal" set of codes (those that give the lowest possible PAPR), according to the number of active user in the system (Ochiai & Imai, 1998; Kang et al., 2002; Alsusa & Yang, 2006).

In this chapter, we further explore a PAPR reduction technique previously proposed by the authors, namely the User Reservation (UR) approach (Paredes Hernández & García Otero, 2009). The UR technique is based on the addition of peak-reducing signals to the signal to be transmitted; these new signals are selected so that they are orthogonal to the original signal and therefore can be removed at the receiver without the need of transmitting any side information and, ideally, without penalizing the bit error rate (BER). In the UR method, these peak-reducing signals are built by using spreading codes that are either dynamically selected from those users that are known to be idle, or deliberately reserved *a priori* for PAPR reduction purposes.

The concept of adding orthogonal signals for peak power mitigation has been previously proposed to reduce PAPR in Discrete MultiTone (DMT) and OFDM transmissions (Tellado & Cioffi, 1998; Gatherer & Polley, 1997), and also in CDMA downlink systems (Väänanen et al., 2002). However, the implementation of this idea in the context of MC-CDMA communications poses particular problems that are discussed in this chapter. Our aim is also to develop strategies to alleviate the inherent complexity of the underlying minimization problem.

2. PAPR properties of MC-CDMA signals

In an MC-CDMA system, a block of M information symbols from each active user are spread in the frequency domain into $N = LM$ subcarriers, where L represents the spreading factor. This is accomplished by multiplying every symbol of the block for user k (where $k \in \{0, 1, \ldots, L-1\}$) by a spreading code $\{c_l^{(k)}, l = 0,1,\ldots,L-1\}$, selected from an set of L orthogonal sequences, thus allowing a maximum of L simultaneous users to share the same radio channel. The spreading codes are the usual Walsh-Hadamard (WH) sequences, which are the columns of the Hadamard matrix of order L, $\mathbf{C}_L$. For L a power of 2, the Hadamard matrix is constructed recursively as

$$\mathbf{C}_2 = \begin{bmatrix} 1 & 1 \\ 1 & -1 \end{bmatrix} \tag{1a}$$

$$\mathbf{C}_n = \mathbf{C}_{n/2} \otimes \mathbf{C}_2 \quad \text{for } n = 4,8,\ldots,L/2,L \tag{1b}$$

where the symbol $\otimes$ denotes the Kronecker tensor product.

We will assume in the sequel that, of the L maximum users of MC-CDMA system, only $K_A < L$ are "active", i.e., are transmitting information symbols, while the other $K_I = L - K_A$ remain inactive or "idle". We will further assume that there is a "natural" indexing for all the users based on their WH codes, being the index associated to a given user the number of the column that its code sequence occupies in the order-L Hadamard matrix. For notational convenience, we will assume that column numbering begins at 0, so that

$$\mathbf{C}_L = \left[\mathbf{c}_L^{(0)} \quad \mathbf{c}_L^{(1)} \quad \cdots \quad \mathbf{c}_L^{(L-1)} \right] \tag{2}$$

with $\mathbf{c}_L^{(k)} = \left[c_0^{(k)}, c_1^{(k)}, \ldots, c_{L-1}^{(k)}\right]^T$ and $(\cdot)^T$ denotes transpose. In this situation, the indices of the active users belong to a set Ω_A, while the indices of the inactive users constitute a set Ω_I. The cardinals of the sets Ω_A and Ω_I are, thus, K_A and K_I, respectively.

In the downlink transmitter, the data symbols of the K_A active users are spread by their specific WH sequences and added together. The complex envelopes are then interleaved in the frequency domain, so that the baseband transmitted signal is

$$s(t) = \sum_{k \in \Omega_A} \sum_{l=0}^{L-1} \sum_{m=0}^{M-1} a_m^{(k)} c_l^{(k)} e^{j2\pi(Ml+m)t/T}, \quad 0 \le t < T \tag{3}$$

where $\{a_m^{(k)}, m = 0,1,\ldots,M-1\}$ are the data symbols in the block for the kth active user and T is the duration of the block. Actually, the modulation of the subcarriers is performed in discrete-time by means of an Inverse Fast Fourier Transform (IFFT).

The PAPR of a signal can be defined as the ratio of peak envelope power to the average envelope power

$$PAPR = \frac{\max_{0 \le t < T} |s(t)|^2}{E[|s(t)|^2]} \tag{4}$$

where $E(\cdot)$ represents the expectation operation, and $E[|s(t)^2|]$ is the average power of $s(t)$. In practice, the computation of the peak power is performed on the discrete-time version of $s(t)$.

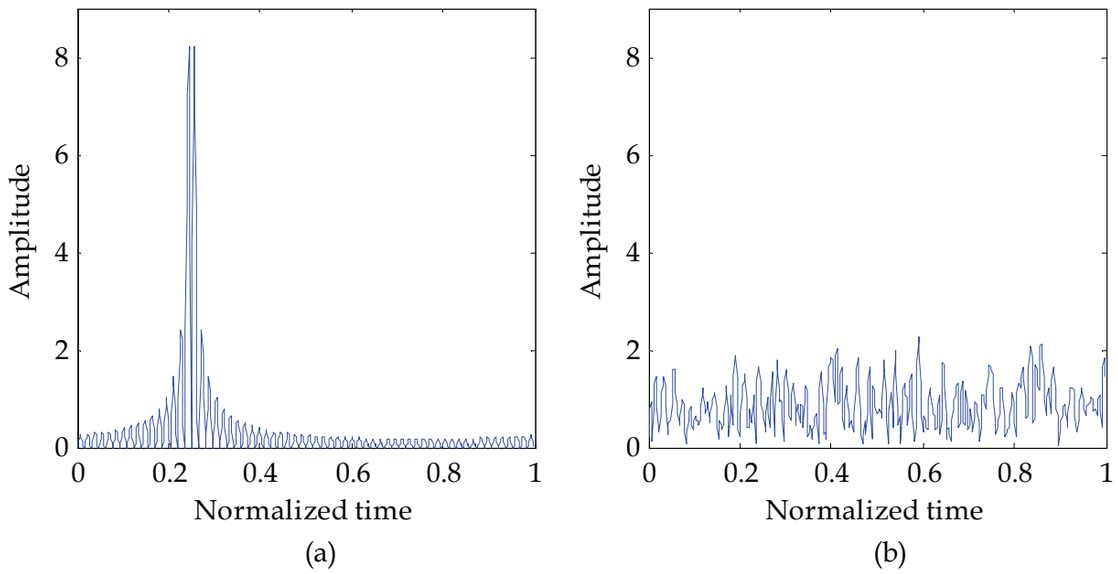


Fig. 1. Examples of amplitude envelopes in MC-CDMA. (a) Single user. (b) Full load

As the PAPR is a random variable, an adequate statistic is needed to characterize it. A common choice is to use the Complementary Cumulative Distribution Function (CCDF), which is defined as the probability of the PAPR exceeding a given threshold

$$CCDF(x) = \Pr(PAPR > x) \tag{5}$$

It should be noticed that the distribution of the PAPR of MC-CDMA signals substantially differs from other multicarrier modulations. For instance, in OFDM schemes, the subcarrier complex envelopes can be assumed to be independent random variables, so that, by applying the Central Limit Theorem, the baseband signal is usually assumed to be a complex Gaussian process. However, in MC-CDMA the subcarrier envelopes generally exhibit strong dependencies, because of the poor autocorrelation properties of WH codes. This fact, in turn, translates into a baseband signal that is no longer Gaussian-like, but instead has mostly low values with sharp peaks at regular intervals. This effect is particularly evident when the number of K_A active users is low.
Fig. 1 shows examples of amplitude envelopes for an MC-CDMA system, with L=32 and M=4 (N=128 subcarriers), and where the two extreme conditions are considered, single user (K_A=1) and full load (K_A=32).
We can see from Fig. 1 that we should expect higher PAPR values as the load of the system decreases.

3. PAPR reduction by user reservation

Our approach to PAPR reduction is based on "borrowing" some of the spreading codes of the inactive users set, so that an adequate linear combination of these codes is added to the active users before the IDFT operation. The coefficients of such linear combination ("pseudo-symbols") should be chosen so that the peaks of the signal are reduced in the time domain. As the added signals are orthogonal to the original ones, the whole process is transparent at the receiver side.

3.1 System model

Fig.2 shows a block diagram of the proposed MC-CDMA downlink transmitter. We can see that the binary information streams of the K_A active users are first converted into sequences of symbols belonging to a QAM constellation, and the symbol sequence of each user is subsequently spread by its unique code. Notice also from Fig.2 that, unlike a conventional MC-CDMA system, the codes belonging to the left K_I inactive users are also used to spread a set of pseudo-symbols computed from the current active users' symbols, and then the whole set of spread sequences are added together before the frequency-domain interleaving and OFDM modulation steps.
With the addition of K_I inactive users for PAPR reduction purposes, our MC-CDMA downlink complex envelope signal for $0 \le t < T$, can be expressed as

$$s(t) = \sum_{k\in\Omega_A}\sum_{l=0}^{L-1}\sum_{m=0}^{M-1} a_m^{(k)} c_l^{(k)} e^{j2\pi(Ml+m)t/T} + \sum_{k\in\Omega_I}\sum_{l=0}^{L-1}\sum_{m=0}^{M-1} a_m^{(k)} c_l^{(k)} e^{j2\pi(Ml+m)t/T} \tag{6}$$

If we sample $s(t)$ at multiples of $T_s=T/NQ$, where Q is the oversampling factor, we will obtain the discrete-time version of (6), which can be rewritten in vector notation as

$$\mathbf{s} = \mathbf{W}_{NQ}^{N}\left(\mathbf{C}_L^A \otimes \mathbf{I}_M\right)\mathbf{a}^A + \mathbf{W}_{NQ}^{N}\left(\mathbf{C}_L^I \otimes \mathbf{I}_M\right)\mathbf{a}^I \tag{7}$$

where the components of vector $\mathbf{s}$ are the NQ samples of the baseband signal $s(t)$ in the block, $\{s_n \equiv s(nT_s), n=0,1,\ldots,NQ-1\}$, $\mathbf{a}^A$ is the vector of K_AM symbols of the K_A active users to be

transmitted, $\mathbf{a}^I$ is the vector of $K_I M$ pseudo-symbols of the K_I idle users to be determined, $\mathbf{W}_{NQ}^{N}$ is a $NQ \times N$ matrix formed by the first N columns of the Inverse Discrete Fourier Transform (IDFT) matrix of order NQ

$$\mathbf{W}_{NQ}^{N} = \begin{bmatrix} 1 & 1 & \cdots & 1 \\ 1 & e^{j2\pi\frac{1\times 1}{NQ}} & \cdots & e^{j2\pi\frac{1\times(N-1)}{NQ}} \\ \vdots & \vdots & \ddots & \vdots \\ 1 & e^{j2\pi\frac{(NQ-1)\times 1}{NQ}} & \cdots & e^{j2\pi\frac{(NQ-1)\times(N-1)}{NQ}} \end{bmatrix} \tag{8}$$

$\mathbf{C}_L^A$ is a $L \times K_A$ matrix whose columns are the WH codes of the active users, $\mathbf{C}_L^I$ is a $L \times K_I$ matrix whose columns are the WH codes of the idle users, and $\mathbf{I}_M$ is the identity matrix of order M.

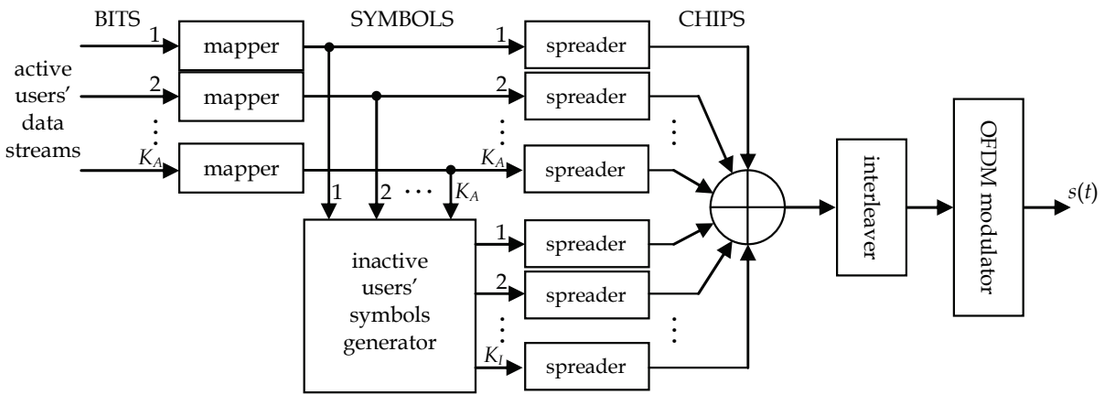


Fig. 2. MC-CDMA downlink transmitter with addition of idle users for PAPR reduction

Thus, our objective is to find the values of the pseudo-symbols $\mathbf{a}^I$ that minimize the peak value of the amplitudes of the components of vector $\mathbf{s}$ in (7).

3.2 Quadratic programming method

Our optimization problem can be formulated as

$$\min_{\mathbf{a}^I} \max_{0\le n\le NQ-1} \left|s(nT_s)\right| = \min_{\mathbf{a}^I} \left\|\mathbf{s}\right\|_\infty = \min_{\mathbf{a}^I} \left\|\mathbf{H}^A\mathbf{a}^A + \mathbf{H}^I\mathbf{a}^I\right\|_\infty \tag{9}$$

where $\|\cdot\|_\infty$ denotes ℓ_∞ norm, and $\mathbf{H}^A$ and $\mathbf{H}^I$ are, respectively, the following $NQ \times K_A M$ and $NQ \times K_I M$ matrices:

$$\mathbf{H}^A = \mathbf{W}_{NQ}^{N}\left(\mathbf{C}_L^A \otimes \mathbf{I}_M\right) \tag{10a}$$

$$\mathbf{H}^I = \mathbf{W}_{NQ}^{N}\left(\mathbf{C}_L^I \otimes \mathbf{I}_M\right) \tag{10b}$$

The minimization involved in (9) may be formulated as a Second-Order Cone Programming (SOCP) convex optimization problem (Sousa et al., 1998)

$$\begin{aligned} &\text{minimize} && z \\ &\text{subject to} && |s_n| \le z,\ 0 \le n \le NQ-1, \\ & && \mathbf{s}=\mathbf{H}^{A}\mathbf{a}^{A}+\mathbf{H}^{I}\mathbf{a}^{I} \\ &\text{in variables} && z \in \mathbb{R},\ \mathbf{a}^{I} \in \mathbb{C}^{K_I M} \end{aligned} \tag{11}$$

Solving (11) in real-time can be a daunting task and we are, thus, interested in reducing the complexity of the optimization problem. Two approaches will be explored in the sequel:

a. Reducing the dimension of the optimization variable $\mathbf{a}^I$.
b. Using suboptimal iterative algorithms to approximately solve (11).

4. Dimension reduction

We will see in the next subsections that not all the inactive users are necessary to enter the system in (6) to reduce the PAPR. This is a consequence of the specific structure of the Hadamard matrices.

4.1 Periodic properties of WH sequences

The particular construction of Hadamard matrices imposes their columns to follow highly structured patterns, thus making WH codes to substantially depart from ideal pseudo-noise (PN) sequences. The most important characteristic of WH sequences that affects their Fourier properties is the existence of inner periodicities, i.e., groups of binary symbols (1 or –1) that are replicated along the whole length of the code. This periodic behavior of WH codes in the frequency domain leads to the appearance of characteristic patterns in the time domain, with many zero values that give the amplitude of the resulting signal a "peaky" aspect (see Fig 1a). This somewhat "sparse" nature of the IDFT of WH codes is, in turn, responsible of the high PAPR values we usually find in MC-CDMA signals.

For the applicability of our UR technique, it is important to characterize the distribution of the peaks in the IDFTs of WH codes. This is because PAPR reduction is possible only if we add in (7) those inactive users whose WH codes have time-domain peaks occupying exactly the same positions as those of the active users, so that, with a suitable choice of the pseudo-symbols, a reduction of the amplitudes of the peaks is possible. As we will see, this characterization of WH sequences will lead us to group them in sets of codes, where the elements of a given set share the property that any idle user with a code belonging to the set can be used to reduce the peaks produced by other active users with codes of the same set.

A careful inspection of the recursive algorithm (1) for generating the Hadamard matrix of order n, $\mathbf{C}_n$ (with n a power of two), shows that two columns of this matrix are generated using a single column of the matrix of order $n/2$, $\mathbf{C}_{n/2}$. If we denote as $\mathbf{c}_{n/2}^{(k)}$ the kth column of $\mathbf{C}_{n/2}$ ($k = 0, 1, \ldots, n/2-1$), it can be seen that the two columns of the matrix $\mathbf{C}_n$ generated by $\mathbf{c}_{n/2}^{(k)}$ are, respectively:

$$\mathbf{c}_n^{(k)} = \begin{bmatrix} \mathbf{c}_{n/2}^{(k)} \\ \mathbf{c}_{n/2}^{(k)} \end{bmatrix}, \qquad k = 0,1,\ldots,n/2-1 \tag{12a}$$

$$\mathbf{c}_n^{(n/2+k)} = \begin{bmatrix} \mathbf{c}_{n/2}^{(k)} \\ -\mathbf{c}_{n/2}^{(k)} \end{bmatrix}, \quad k = 0,1,\ldots,n/2-1 \tag{12b}$$

We can see from (12a) that the columns of the Hadamard matrix of order $n/2$ are simply repeated twice to form the first $n/2$ columns of the Hadamard matrix of order n. This, in turn, has two implications:

Assertion 1. Any existing periodic structure in $\mathbf{c}_{n/2}^{(k)}$ is directly inherited by $\mathbf{c}_{n}^{(k)}$.

Assertion 2. In case $\mathbf{c}_{n/2}^{(k)}$ has no inner periodicity, a new repetition pattern of length $n/2$ is created in $\mathbf{c}_{n}^{(k)}$.

On the other hand, (12b) implies that the last $n/2$ columns of the order n Hadamard matrix are formed by appending to the columns of the order $n/2$ matrix these same columns but with the sign of their elements changed; therefore, the periodicities in the columns of the original matrix are now destroyed by the copy-and-negate operation in the last $n/2$ columns. Nevertheless, we can easily see that (12b), when iterated in alternation with (12a), introduces another significant effect:

Assertion 3. Any repetitive structure in $\mathbf{c}_{n}^{(k)}$ is always composed of two equal-length consecutive substructures with opposite signs.

If we denote as P the minimum length of a pattern of binary symbols that is repeated an integer number of times along any given column of the Hadamard matrix of order n (period length), we can see by inspection that the first column (formed by n 1s) has $P=1$ and the second column (formed by a repeated alternating pattern of 1s and -1s) has $P=2$, respectively; then, by recursively applying assertions 1 and 2, we can build the following table:

WH code index	Period
0	1
1	2
2, 3	4
4 to 7	8
⋮	⋮
$L/4$ to $L/2-1$	$L/2$
$L/2$ to $L-1$	L

Table 1. Periods of the WH codes of length L

Notice from Table 1 that, for an Lth order Hadamard matrix, we will have $\log_2 L+1$ different periods in its columns. Notice also that, for $P>1$, as the period is doubled the number of WH sequences with the same period length is also doubled.

4.2 Selection of inactive users

The periodic structure of the WH codes determines their behavior in the time domain, because the number and positions of the non-zero values of the IDFT of a sequence directly depends on the value of its period P. To illustrate this fact, Fig. 3 shows the sampled amplitude envelopes of the signals obtained in a single-user MC-CDMA transmitter with two different WH codes (corresponding to different columns of the Hadamard matrix $\mathbf{C}_L$)

Notice from Fig.3 that users whose codes have low indices tend to produce few scattered peaks in the time domain, while users using codes with higher values in their indices generate a high number of non-zero values in the time domain.

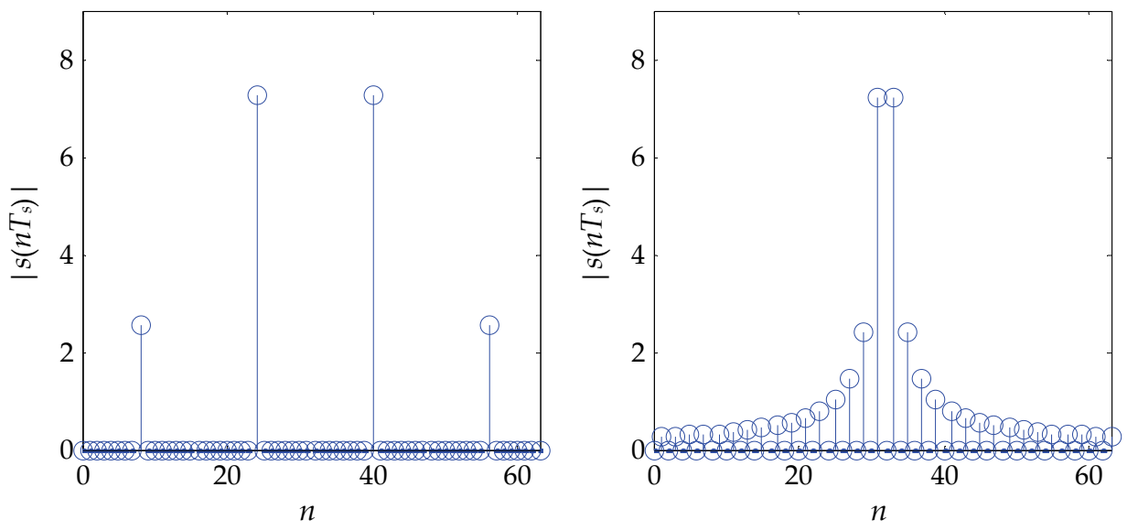


Fig. 3. Samples of the envelope of an MC-CDMA signal for a single user and different WH codes. (a) k=2. (b) k=16

It is clear from Fig. 3 that idle users can only mitigate the PAPR of signals generated by active users with the same periodic patterns in their codes. This is because only those users will be able to generate signals with their peaks located in the same time instants (and with opposite signs) as the peaks of the active users, so that these latter peaks can be reduced. Therefore we conclude that we will include in (11) only those idle users whose WH codes have the same period as any of the active users currently in the system; the choice of inactive users can be easily obtained with the help of Table 1, and the selection rule can be summarized as follows:

For every active user $k_A \in \Omega_A$ (with $k > 1$), select for the optimization (11) only the inactive users $k_I \in \Omega_I$ such that $\lfloor \log_2 k_I \rfloor = \lfloor \log_2 k_A \rfloor$, where $\lfloor \cdot \rfloor$ denotes the "integer part".

5. Iterative clipping approaches

The SOCP optimization of (11) solved with interior-point methods requires $O((NQ)^{3/2})$ operations (Sousa et al, 1998). Although the structure of the matrices involved could be exploited to reduce the complexity, it is desirable to devise simpler suboptimal algorithms whose complexity only grows linearly with the number of subcarriers. This can be accomplished if we adopt a strategy of iterative clipping of the time-domain signal, so that, at the ith iteration, the signal vector is updated as

$$\mathbf{s}^{(i+1)} = \mathbf{s}^{(i)} + \mathbf{r}^{(i)} \tag{13}$$

where $\mathbf{r}^{(i)}$ is a "clipping vector" that is designed to reduce the magnitude of one or more of the samples of the signal vector. Notice that, as the clipping vector should cause no interference to the active users, it must be generated as

$$\mathbf{r}^{(i)} = \mathbf{H}^I \mathbf{b}^{(i)} \tag{14}$$

where $\mathbf{H}^{I}$ is defined in (10b) and $\mathbf{b}^{(i)} \in \mathbb{C}^{K_I M}$.
Now suppose that, at the ith iteration, we want to clip the set of samples of vector $\mathbf{s}^{(i)}$ $\{s_u^{(i)}, u \in U^{(i)}\}$, where $U^{(i)}$ is a subset of the indices $\{0, 1, \ldots, NQ-1\}$. Thus, in (13) we would like the clipping vector $\mathbf{r}^{(i)}$ to reduce the magnitudes of those samples without modifying other values in vector $\mathbf{s}^{(i)}$, so the *ideal* clipping vector should be of the form

$$\widehat{\mathbf{r}}^{(i)} = \sum_{u \in U^{(i)}} \alpha_u^{(i)} \boldsymbol{\delta}_u \tag{15}$$

where $\boldsymbol{\delta}_u$ is the length-NQ discrete-time impulse delayed by u samples

$$\boldsymbol{\delta}_u = [\underbrace{0,0,\ldots,0}_{u},1,\underbrace{0,0,\ldots,0}_{NQ-u-1}]^T \tag{16}$$

and $\{\alpha_u^{(i)}, u \in U^{(i)}\}$ is a set of suitably selected complex coefficients.
Notice, however, that, as we require vector $\mathbf{r}^{(i)}$ to be of the form (14) it is not possible, in general, to synthesize the set of required time-domain impulses using only symbols from the inactive users, so $\boldsymbol{\delta}_u$ must be replaced by another vector $\mathbf{d}_u$ generated as

$$\mathbf{d}_u = \mathbf{H}^{I} \mathbf{b}_u \tag{17}$$

so that the actual clipping vector would result in

$$\mathbf{r}^{(i)} = \sum_{u \in U^{(i)}} \alpha_u^{(i)} \mathbf{d}_u \tag{18}$$

which can be easily shown to be in agreement with restriction (14), with $\mathbf{b}^{(i)}$ obtained as

$$\mathbf{b}^{(i)} = \sum_{u \in U^{(i)}} \alpha_u^{(i)} \mathbf{b}_u \tag{19}$$

A straightforward way to approximate the impulse vector $\boldsymbol{\delta}_u$ is by minimizing a distance between vectors $\boldsymbol{\delta}_u$ and $\mathbf{d}_u$

$$\mathbf{b}_u = \arg\min_{\mathrm{b}} \left\| \mathbf{H}^{I} \mathbf{b} - \boldsymbol{\delta}_u \right\|_p \tag{20}$$

where $\| \cdot \|_{\mathrm{p}}$ denotes the p-norm. When $p = 2$, we have the conventional least-squares (LS) solution

$$\mathbf{b}_u = (\mathbf{H}^{I*}\mathbf{H}^{I})^{-1}\mathbf{H}^{I*}\boldsymbol{\delta}_u = \frac{1}{LNQ}\mathbf{H}^{I*}\boldsymbol{\delta}_u \tag{21}$$

where $(\cdot)^*$ denotes conjugate transpose and we used the fact: $\mathbf{H}^{I*}\mathbf{H}^{I} = LNQ\mathbf{I}_{K_I M}$. Replacing (21) in (17), we arrive at

$$\mathbf{d}_u = \mathbf{H}^{I}\mathbf{b}_u = \frac{1}{LNQ}\mathbf{H}^{I}\mathbf{H}^{I*}\boldsymbol{\delta}_u \tag{22}$$

so that $\mathbf{d}_u$ is the orthogonal projection of the impulse vector onto the subspace spanned by the columns of $\mathbf{H}^I$. Now, taking into account from (16) that $\boldsymbol{\delta}_u$ is just the uth column of $\mathbf{I}_{NQ}$, we conclude that the LS approximation to the unit impulse vector centered at position u is the uth column of the projection matrix

$$\mathbf{P}^I = \frac{1}{LNQ}\mathbf{H}^I\mathbf{H}^{I*} \tag{23}$$

Notice that, in general, matrix $\mathbf{P}^I$ of (23) is not a circulant matrix. This is in contrast with the POCS approach for PAPR mitigation in OFDM (Gatherer and Polley, 1997) and related methods, where the functions used for peak reduction are obtained by circularly shifting and scaling a single basic clipping vector. Of course, other norms can be chosen in the optimization (20). For instance, for $p = \propto$, the problem of finding the optimal vector $\mathbf{b}_u$ can be also cast as a SOCP. Notice that the set of vectors $\{\mathbf{d}_u, u \in U^{(i)}\}$ is pre-computed and stored off-line, and so the complexity of solving (20) is irrelevant.

Fig. 4 shows examples of the approximations to a discrete-time impulse we get using (20) and (17) for $p = 2$ and $p = \propto$, respectively. We can see that the minimization of the ℓ_2 norm produces a signal that has spurious peaks with very high amplitudes; therefore, the addition of this approximate impulse to the original signal will induce the emergence of new peaks that need to be clipped, thus slowing the convergence of any iterative procedure.

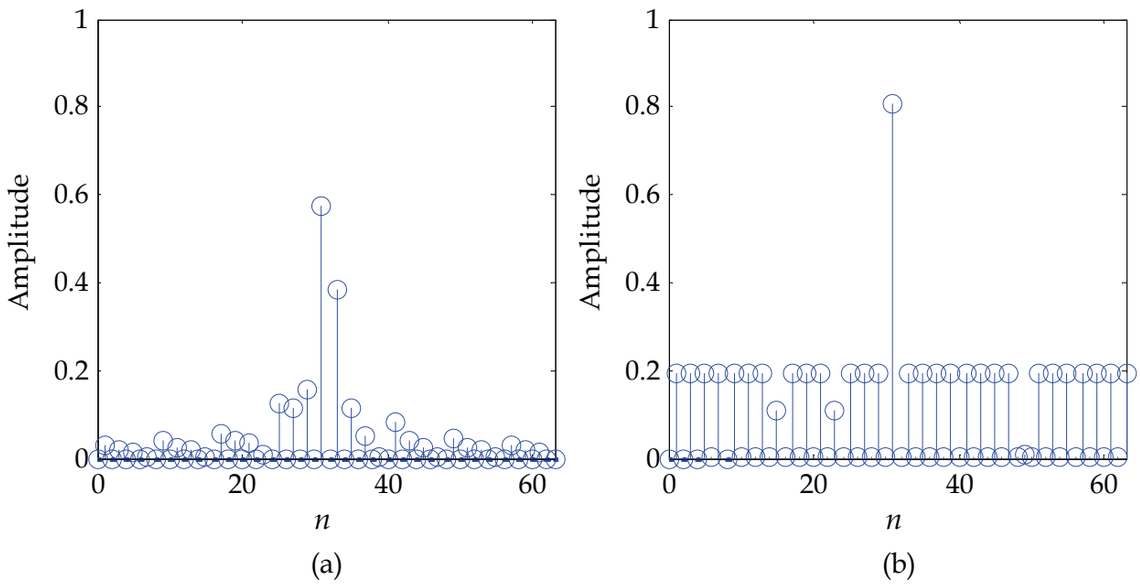


Fig. 4. Approximations to a discrete-time impulse using only inactive users. (a) Minimizing ℓ_2 norm. (b) Minimizing ℓ_∞ norm

Several approaches can be found in the literature for the iterative minimization of the PAPR in OFDM based on tone reservation. Among those, the two most popular are probably the SCR-gradient method (Tellado and Cioffi, 1998) and the active-set approach (Krongold, 2004). Both can be readily adapted to simplify the UR method for PAPR reduction in MC-CDMA as we will see in the sequel.

5.1 SCR-gradient

Following (Tellado & Cioffi, 1998), we define the clipping or soft limiter (SL) operator

$$clip(s_n) = \begin{cases} s_n, & |s_n| \le A \\ A\dfrac{s_n}{|s_n|}, & |s_n| > A \end{cases} \tag{24}$$

with $A > 0$. Now, if all the components $\{s_n,\ n=0,1,\ldots,NQ-1\}$ of a given signal vector $\mathbf{s}$ are transformed by an SL, we can define the clipping noise as

$$\mathbf{z} = \mathbf{s} - clip(\mathbf{s}) \tag{25}$$

If inactive users are added to the original signal $\mathbf{s}^A$ (generated using only the symbols of the active users), so that the model for the clipped signal $\mathbf{s}$ is

$$\mathbf{s} = \mathbf{s}^A + \mathbf{s}^I = \mathbf{H}^A\mathbf{a}^A + \mathbf{H}^I\mathbf{a}^I \tag{26}$$

now the vector of pseudo-symbols of the inactive users $\mathbf{a}^I$ can be designed to reduce the clipping noise. To accomplish this, we define the signal to clipping noise power ratio (SCR) as

$$SCR = \frac{\mathbf{s}^{A*}\mathbf{s}^A}{\mathbf{z}^*\mathbf{z}} \tag{27}$$

The maximization of the SCR in (27) leads to a minimization of its denominator (the clipping noise power). This latter can be written, using (25), (26) and (24), and after some manipulations as:

$$\mathbf{z}^*\mathbf{z} = \sum_{|s_u|>A} \left(|s_u| - A\right)^2 \tag{28}$$

with

$$s_u = s_u^A + \boldsymbol{\delta}_u^T\mathbf{H}^I\mathbf{a}^I \tag{29}$$

where $\boldsymbol{\delta}_u$ was defined in (16). Now, instead of a direct minimization of (28) with respect to $\mathbf{a}^I$, we will try an iterative algorithm based on the gradient of the clipping noise power of the form:

$$\mathbf{a}^{I(i+1)} = \mathbf{a}^{I(i)} - \mu\nabla_{\mathbf{a}^{I(i)}}\left(\mathbf{z}^*\mathbf{z}\right) \tag{30}$$

where $\mu > 0$ and ∇ is the complex gradient operator (Haykin, 1996). Using (28) and (29), the gradient vector can be shown to be

$$\nabla_{\mathbf{a}^I}\left(\mathbf{z}^*\mathbf{z}\right) = 2\sum_{|s_u|>A}\left(1 - A/|s_u|\right)s_u\mathbf{H}^{I*}\boldsymbol{\delta}_u \tag{31}$$

According to (26), the recursion for the pseudo-symbols (30) can be equivalently translated to the signal vector

$$\mathbf{s}^{(i+1)} = \mathbf{s}^{(i)} - \mu \mathbf{H}^{I} \nabla_{\mathbf{a}^{I(i)}} \left(\mathbf{z}^{*} \mathbf{z} \right) \tag{32}$$

So that, substituting (31) in (32), and taking into account (22), we finally arrive at

$$\mathbf{s}^{(i+1)} = \mathbf{s}^{(i)} - \mu' \sum_{\left|s_u^{(i)}\right| > A} \left(1 - A / \left|s_u^{(i)}\right| \right) s_u^{(i)} \mathbf{d}_u \tag{33}$$

where $\mu' = 2\mu LNQ$, which is in agreement with (13) and (18) with

$$\begin{aligned} U^{(i)} &= \left\{ u : \left|s_u^{(i)}\right| > A \right\} \\ \alpha_u^{(i)} &= -\mu' \left(1 - A / \left|s_u^{(i)}\right| \right) s_u^{(i)}, \quad u \in U^{(i)} \end{aligned} \tag{34}$$

Notice that, for $\mu' = 1$ and "ideal" impulses ($\mathbf{d}_u \approx \boldsymbol{\delta}_u$), the signal would be soft-limited in one iteration to the maximum amplitude A.

The main drawbacks of this algorithm are the difficulty of *a priori* fixing a convenient clipping level A, and the probable slow convergence of the algorithm.

5.2 Active-set

The slow convergence of the SCR-gradient method is due to the use of non-ideal impulses $\mathbf{d}_u$ in the clipping process, because they must satisfy restriction (17). As they have non-zero values outside the position of their maximum (see Fig. 4), any attempt to clip a peak of the signal at a given discrete time u using $\mathbf{d}_u$ can potentially give rise to unexpected new peaks at another positions of the signal vector.

On the contrary, the active-set approach (Krongold & Jones, 2004) keeps the maximum value of the signal amplitude controlled, so that it is always reduced at every iteration of the algorithm. An outline of the active-set method follows below (Wang et al, 2008):

1. Find the component of **s** with the highest magnitude (peak value).
2. Clip the signal by adding inactive users so that the peak value is balanced with another secondary peak. Now we have two peaks with the same magnitude, which is lower than the original maximum.
3. Add again inactive users to simultaneously reduce the magnitudes of the two balanced peaks until we get three balanced peaks.
4. Repeat this process until either the magnitudes of the peaks cannot be further reduced significantly or a maximum number of iterations is reached.

Notice that, at the ith stage of the algorithm we have an *active set* $\{s_u^{(i)}, u \in U^{(i)}\}$ of signal peaks that have the same maximum magnitude, i.e.:

$$\begin{aligned} |s_u^{(i)}| &= A^{(i)}, \quad \text{if } u \in U^{(i)} \\ |s_u^{(i)}| &< A^{(i)}, \quad \text{if } u \in \bar{U}^{(i)} \end{aligned} \tag{35}$$

where $A^{(i)}$ is the peak magnitude and $\bar{U}^{(i)}$ is the complement of the set $U^{(i)}$. The problem at this point is, thus, to find a clipping vector $\mathbf{r}^{(i)}$ generated as (18) that, when added to the signal $\mathbf{s}^{(i)}$ as in (13), will satisfy two conditions:

a. The addition of the clipping vector must keep the magnitudes of the components of the current active set balanced.

b. The addition of the clipping vector should reduce the value of the peak magnitude until it reaches the magnitude of a signal sample that was previously outside the active set.

Both conditions can be easily met if we design the vector $\mathbf{r}^{(i)}$ in two stages: first, we obtain a vector $\mathbf{q}^{(i)}$ as a suitable combination of non-ideal impulses of the form (17) that satisfies condition a)

$$\mathbf{q}^{(i)} = \sum_{u \in U^{(i)}} \beta_u^{(i)} \mathbf{d}_u \tag{36}$$

and then, we compute a real number to scale vector $\mathbf{q}^{(i)}$ until condition b) is met. Therefore, the final update equation for the signal vector is

$$\mathbf{s}^{(i+1)} = \mathbf{s}^{(i)} + \mu^{(i)} \mathbf{q}^{(i)} \tag{37}$$

where $\mu^{(i)}$ is a convenient step-size.

A simple way to ensure that $\mathbf{q}^{(i)}$ satisfies condition a) is to force its components at the locations of the peaks to be of unit magnitude and to have the opposite signs to the signal peaks in the current active set

$$q_u^{(i)} = -\frac{s_u^{(i)}}{|s_u^{(i)}|} = -\frac{s_u^{(i)}}{A^{(i)}}, \quad u \in U^{(i)} \tag{38}$$

because then, according to (35), (37) and (38):

$$A^{(i+1)} = \left|s_u^{(i+1)}\right| = \left|s_u^{(i)} - \mu^{(i)} \frac{s_u^{(i)}}{A^{(i)}}\right| = \left|A^{(i)} - \mu^{(i)}\right|, \quad u \in U^{(i)} \tag{39}$$

So, taking into account (36) and (38), the set of coefficients $\{\beta_u^{(i)}, u \in U^{(i)}\}$ is obtained as the solution of a system of linear equations

$$\sum_{v \in U^{(i)}} d_{u,v} \beta_v^{(i)} = -\frac{s_u^{(i)}}{A^{(i)}}, \quad u \in U^{(i)} \tag{40}$$

where $d_{u,v}$ is the vth component of vector $\mathbf{d}_u$.

Once the vector $\mathbf{q}^{(i)}$ is computed, the step-size $\mu^{(i)}$ is determined by forcing the new peak magnitude $A^{(i+1)}$ to be equal to the highest magnitude of the components of $\mathbf{s}^{(i+1)}$ not in the current active set

$$A^{(i+1)} = \max_{n \in \bar{U}^{(i)}} \left|s_n^{(i+1)}\right| \tag{41}$$

So, we can consider the possible samples to be included in the next active set $\{s_n^{(i)}, n \in \bar{U}^{(i)}\}$ and associate a candidate positive step-size $\{\mu_n^{(i)} > 0, n \in \bar{U}^{(i)}\}$ to each of them. According to (39) and (37), the candidates verify the conditions

$$\left|A^{(i)} - \mu_n^{(i)}\right| = \left|s_n^{(i)} + \mu_n^{(i)} q_n^{(i)}\right|, \quad n \in \bar{U}^{(i)} \tag{42}$$

so that we select as step-size the minimum of all the candidates

$$\mu^{(i)} = \min\left\{\mu_n^{(i)}, n \in \bar{U}^{(i)}\right\} \tag{43}$$

and its associated signal sample enters the new active set. This choice ensures that no other sample exceeds the magnitude of the samples in the current active set because we have the smallest possible reduction in the peak magnitude.

Squaring (42) and rearranging terms, we find that $\mu_n^{(i)}$ satisfies a quadratic equation with two real roots, so we choose for $\mu_n^{(i)}$ the smallest positive root, given by (Erdogan, 2006)

$$\mu_n^{(i)} = \frac{\psi_n^{(i)} - \sqrt{\psi_n^{(i)2} - \xi_n^{(i)}\zeta_n^{(i)}}}{\xi_n^{(i)}} \tag{44}$$

with

$$\begin{aligned} \xi_n^{(i)} &= 1 - |\, q_n^{(i)} \,|^2 \\ \psi_n^{(i)} &= A^{(i)} + \Re\{s_n^{(i)} q_n^{(i)*}\} \\ \zeta_n^{(i)} &= A^{(i)2} - |\, s_n^{(i)} \,|^2 \end{aligned} \tag{45}$$

where $\Re(\cdot)$ denotes real part. The overall complexity of the active-set method can be alleviated if we reduce the number of possible samples to enter the active set, so that we need to compute only a small number of candidate step-sizes. For instance, in (Wang et al, 2008) the authors propose a technique based on the prediction at the *i*th stage of a tentative step-size $\hat{\mu}^{(i)}$, and so the candidate samples are only those that verify the condition

$$\left|s_n^{(i)} + \hat{\mu}^{(i)} q_n^{(i)}\right| > A^{(i)} - \hat{\mu}^{(i)}, \quad n \in \bar{U}^{(i)} \tag{46}$$

6. Experimental results

The performance of the UR algorithm was tested by simulating the system of Fig. 2 under the conditions listed in Table 2

Modulation	QPSK
Spreading codes	Walsh-Hadamard
Spreading factor (*L*)	32
Data symbols per user in a frame (*M*)	4
Number of subcarriers (*N*)	128
Oversampling factor (*Q*)	4

Table 2. Simulation parameters

The transformation of the signal in the time-domain induced by the UR method is illustrated in Fig.5, which depicts the amplitude of the signal to be transmitted for an MC-CDMA system with only one active user. It can be seen that the value of the peak is substantially reduced with respect to the original signal, and it is also evident from Fig. 3 that the ℓ_∞ norm minimization performed by algorithm (12) forces, in this case, the resulting signal vector to have a characteristic pattern of "equalized" maximum amplitude values.

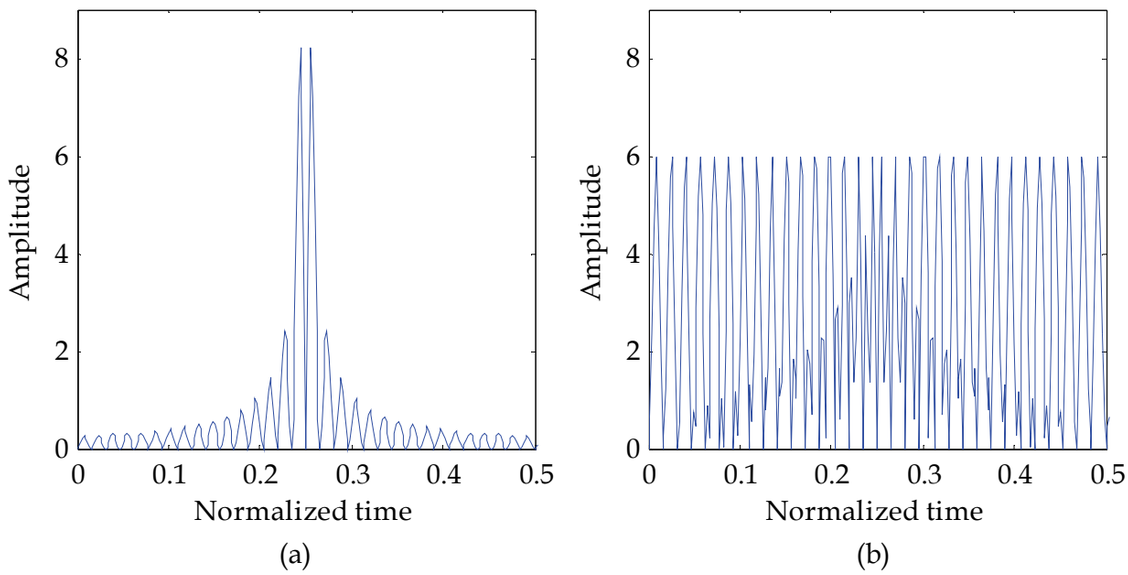
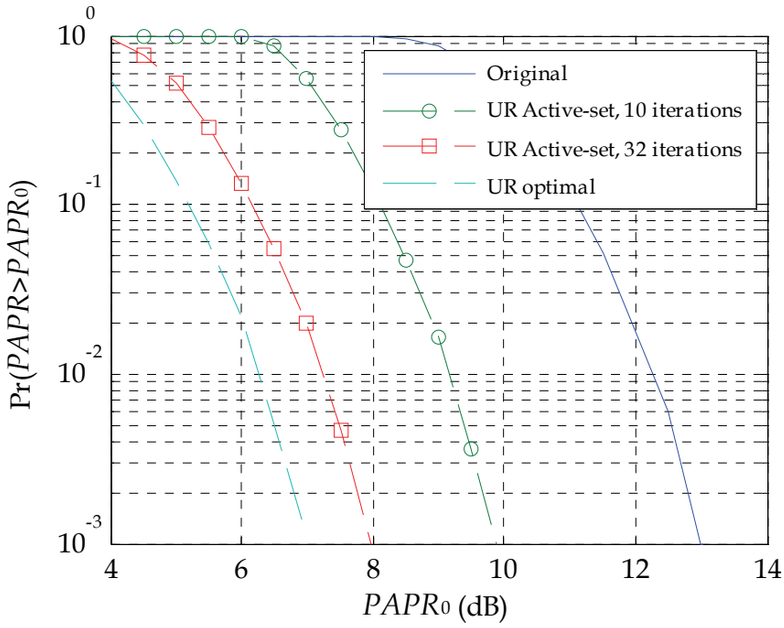


Fig. 5. Examples of amplitude envelopes in MC-CDMA. (a) Original. (b) With peak values reduced via UR

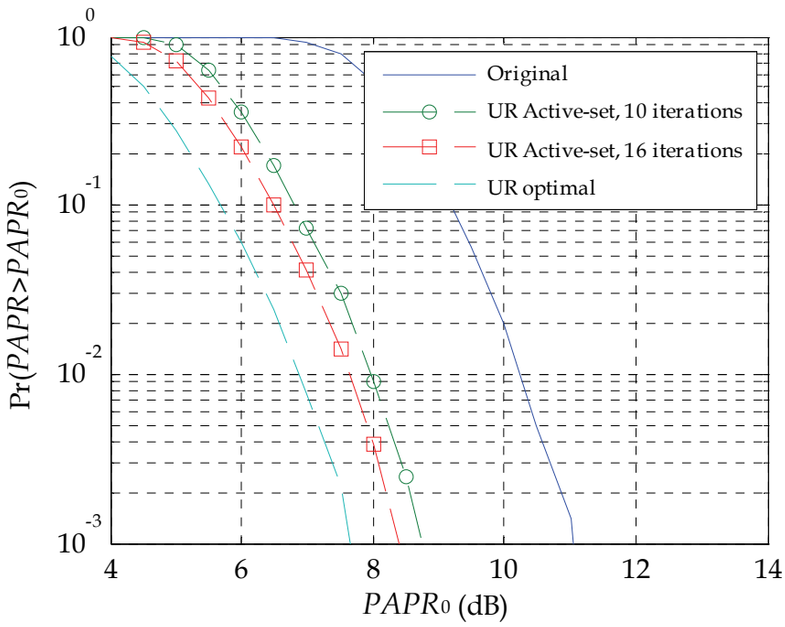
For comparison purposes, Fig. 6 represents the estimated CCDF of the PAPR, as defined in (4) and (5), obtained under two different conditions for the system load: 8 and 24 active users, respectively. The K_A=8 case represents a "low load" situation (for only 25% of the maximum number of users are active), whereas a system with K_A=24 (75% of the maximum) can be considered as highly loaded. In both cases, we have compared the PAPR of the transmitted signal in the original MC-CDMA system with that obtained when the UR method is applied, using either the exact optimization (11) or the suboptimal active-set approach. For the latter algorithm, we have employed in the clipping procedure, represented by (36) and (37), the approximate impulses given by (22).

It is evident from Fig. 6 that, as it was expected, for an unmodified MC-CDMA system described by (3), the PAPR can become very high if the number of active users is small. Notice also that it is precisely in this case (K_A=8) when the PAPR reduction provided by the UR method is most noticeable. That is because, as K_A decreases, more inactive users are available and the dimensionality of vector $\mathbf{a}^I$ in (7) increases, letting more degrees of freedom to the optimization procedure (11).

We can also see from Fig. 6 that the active-set approach gets close to the optimal if a sufficient number of iterations are allowed. Notice that there is an upper bound for this parameter: the number of iterations cannot exceed the size of vector $\mathbf{a}^I$, because then the matrix involved in the linear system (40) becomes singular.



(a)



(b)

Fig. 6. CCDF of the PAPR under different MC-CDMA system loads. (a) Low load (8 active users). (b) High load (24 active users)

7. Conclusions

The UR scheme for the reduction of the PAPR of the signal transmitted in an MC-CDMA downlink is explored in this book chapter. This approach does not require any modification

at the receiver side, because it is based on the addition of the spreading codes of users that are inactive. The optimization procedure provides significant improvements in PAPR, especially when the number of active users is relatively low.
The inherent complexity of the SOCP optimization involved in the method can be alleviated if we select only inactive users with WH codes that share the same periods as those of the active users in the system. For further computational savings, suboptimal procedures can be applied to reduce the PAPR; these are based on the idea of iteratively clipping the original signal in the time domain via the addition of impulse-like signals that are synthesized using the WH codes of inactive users.

8. Acknowledgement

The work presented in this book chapter was partially supported by the Spanish Ministry of Science and Innovation under project no. TEC2009-14219-C03-01.

9. References

Alsusa, E. & Yang, L. (2006). MC-CDMA Specific PAPR Reduction Technique Utilising Spreading Code Redistribution. *IEEE Vehicular Technology Conference (VTC Fall '06)*, Montreal, Canada, pp. 1-5.

Bäuml, R. W.; Fischer, R. F. H. & Huber, J. B. (1996). Reducing the Peak-to-Average Power Ratio of Multicarrier Modulation by Selecting Mapping, *IEE Electronics Letters*, Vol. 32, No. 22, pp. 2056-2057.

Breiling, M.; Müller-Weinfurtner, S. H. & Hubber, J. B. (2001). SLM Peak-Power Reduction Without Explicit Side Information, *IEEE Communications Letters*, Vol. 5, No. 6, pp. 239-241.

Cimini, L. J. & Sollenberger, N. R. (2000). Peak-to-Average Power Ratio Reduction of an OFDM Signal using Partial Transmit Sequences, *IEEE Communications Letters*, Vol. 4, No. 3, pp. 86-88.

Erdogan, A. T. (2006). A Low Complexity Multicarrier PAR Reduction Approach Based on Subgradient Optimization, *Signal Processing*, vol. 86, no. 12, pp. 3890-3903.

Fazel, K. & Kaiser, S. (2008). *Multi-Carrier and Spread Spectrum System: From OFDM and MC-CDMA to LTE and WiMAX*, Second ed. The Atrium, Southern Gate, Chichester, West Sussex PO19 8SQ, England: John Wiley & Sons Ltd.

Gatherer, A. & Polley, M. (1997). Controlling Clipping Probability in DMT Transmission, *Proceedings of the 31st Asilomar Conference on Signals, Systems, and Computers*, vol. 1, pp. 578-584, Pacific Grove, Calif, USA, November 1997.

Han, S. H.; Cioffi, J. M. & Lee, J. H. (2006). Tone Injection with Hexagonal Constellation for Peak-to-Average Power Ratio Reduction in OFDM, *IEEE Communications Letters*, Vol. 10, No. 9, pp. 646-648.

Hara, S. & Prasad, R. (1997). Overview of Multicarrier CDMA, *IEEE Communications Magazine*, Vol. 35, No. 12, pp. 126-133.

Haykin, S. (1996). *Adaptive Filter Theory (3rd ed.)*, Prentice-Hall, Inc., Upper Saddle River, NJ.

Jayalath, A. D. S. & Tellambura, C. (2000). Adaptive PTS Approach for Reduction of Peak-to-Average Power Ratio of OFDM Signals, *IEE Electronics Letters*, Vol. 36, No. 14, pp. 1226-1228.

Jones, A. E.; Wilkinson, T. A. & Barton, S. K. (1994). Block Coding Scheme for Reduction of Peak to Mean Envelope Power Ratio of Multicarrier Transmission Schemes, *IEE Electronics Letters*, Vol. 30, No. 25, pp. 2098-2099.

Kang, K.; Choi, K. & Kim, S. (2002). Reduced Search for Optimum Code Sets to Reduce PAPR in MC-CDMA System. *The 5th International Symposium on Wireless Personal Multimedia Communications*, pp. 135-139.

Krongold, B. S. & Jones, D .L. (2004). An Active-Set Approach for OFDM PAR reduction via Tone Reservation, *IEEE Transactions on Signal Processing,* vol. 52, no. 2, pp. 495- 509.

Li, X. & Cimini, L. J. (1997). Effects of Clipping and Filtering on the Performance of OFDM. *IEEE 47th Vehicular Technology Conference (VTC '97)*, pp. 1634-1638.

Ochiai, H. & Imai, H. (1998). OFDM-CDMA with Peak Power Reduction based on the Spreading Sequences. *IEEE International Communications Conference (ICC '98)*, pp. 1299-1303.

Ohkubo, N. & Ohtsuki, T. (2002). A Peak to Average Power Ratio Reduction of Multicarrier CDMA using Selected Mapping. *IEEE 56th Vehicular Technology Conference (VTC '02)*, pp. 2086-2090.

Paredes Hernandez, L. A. P. & García Otero, M. (2009). User Reservation Approach for Peak-to-Average Power Ratio Reduction in MC-CDMA Systems. *IEEE 69th Vehicular Technology Conference (VTC Spring '09)*, Barcelona, Spain, pp. 1-5.

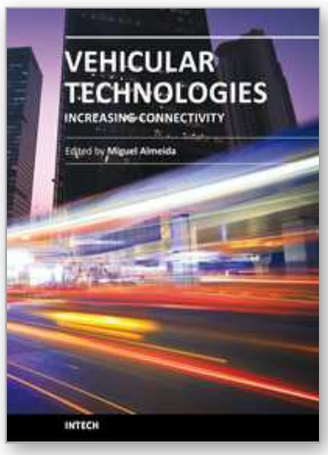
Ruangsurat, N. & Rajatheva, R. M. A. P. (2001). An Investigation of Peak-to-Average Power Ratio in MC-CDMA combined with Partial Transmit Sequence. *IEEE Vehicular Technology Conference (VTC '01)*, pp. 761-765.

Sousa, M.; Vandenberghe, L.; Boyd, S. & Lebret, H. (1998). Applications of Second-Order Cone Programming, *Linear Algebra and its Applications*, vol. 284, pp. 193-228.

Tellado, J. & Cioffi, J. M. (1998). Revisiting DMT's PAR, *ETSI/ANSI TM6, contribution number TD08*.

Väänanen, O.; Vankka, J.; Viero, T. & Halonen, K. (2002). Reducing the Crest Factor of a CDMA Downlink Signal by Adding Unused Channelization Codes, *IEEE Communications Letters*, Vol. 6, No. 10, pp. 443-445.

Wang, M.; Quevedo, D. E.; Goodwin, G. C. & Krongold, B. S. (2008). A Complex-Baseband Active-Set Approach for Tone Reservation PAR Reduction in OFDM Systems, *Australian Communications Theory Workshop, 2008 (AusCTW 2008),* pp. 113-118, Christchurch, New Zealand, Jan. 30 2008-Feb. 1 2008.



Vehicular Technologies: Increasing Connectivity
Edited by Dr Miguel Almeida

ISBN 978-953-307-223-4
Hard cover, 448 pages
Publisher InTech
Published online 11, April, 2011
Published in print edition April, 2011

This book provides an insight on both the challenges and the technological solutions of several approaches, which allow connecting vehicles between each other and with the network. It underlines the trends on networking capabilities and their issues, further focusing on the MAC and Physical layer challenges. Ranging from the advances on radio access technologies to intelligent mechanisms deployed to enhance cooperative communications, cognitive radio and multiple antenna systems have been given particular highlight.

How to reference
In order to correctly reference this scholarly work, feel free to copy and paste the following:

Mariano García Otero and Luis A. Paredes Hernández (2011). Reduced-Complexity PAPR Minimization Schemes for MC-CDMA Systems, Vehicular Technologies: Increasing Connectivity, Dr Miguel Almeida (Ed.), ISBN: 978-953-307-223-4, InTech, Available from: http://www.intechopen.com/books/vehicular-technologies-increasing-connectivity/reduced-complexity-papr-minimization-schemes-for-mc-cdma-systems

INTECH
open science | open minds

InTech Europe
University Campus STeP Ri
Slavka Krautzeka 83/A
51000 Rijeka, Croatia
Phone: +385 (51) 770 447
Fax: +385 (51) 686 166
www.intechopen.com

InTech China
Unit 405, Office Block, Hotel Equatorial Shanghai
No.65, Yan An Road (West), Shanghai, 200040, China
中国上海市延安西路65号上海国际贵都大饭店办公楼405单元
Phone: +86-21-62489820
Fax: +86-21-62489821

© 2011 The Author(s). Licensee IntechOpen. This chapter is distributed under the terms of the Creative Commons Attribution-NonCommercial-ShareAlike-3.0 License, which permits use, distribution and reproduction for non-commercial purposes, provided the original is properly cited and derivative works building on this content are distributed under the same license.

IntechOpen

IntechOpen